IOPscience iopscience.iop.org

Home Search Collections Journals About Contact us My IOPscience

Partially confined excitons in semiconductor nanocrystals with a finite size dielectric interface

This article has been downloaded from IOPscience. Please scroll down to see the full text article.

2001 J. Phys.: Condens. Matter 13 319

(http://iopscience.iop.org/0953-8984/13/2/309)

View the table of contents for this issue, or go to the journal homepage for more

Download details:
IP Address: 171.66.16.226
The article was downloaded on 16/05/2010 at 08:19

Please note that terms and conditions apply.

INSTITUTE OF PHYSICS PUBLISHING JOURNAL OF PHYSICS: CONDENSED MATTER

J. Phys.: Condens. Matter **13** (2001) 319–334 www.iop.org/Journals/cm PII: S0953-8984(01)15470-6

# Partially confined excitons in semiconductor nanocrystals with a finite size dielectric interface

**P G Bolcatto**[1] **and C R Proetto**

Comisión Nacional de Energía Atómica, Centro Atómico Bariloche and Instituto Balseiro, 8400 Bariloche, Argentina

Received 13 July 2000

**Abstract**

The combined effect of finite potential barriers and the dielectric mismatch between dot and matrix on excitonic properties of semiconductor quantum dots has been studied. To avoid the unphysical divergence in the self-polarization energy which arises for the simplest and profusely adopted step-like model of the dielectric interface, we proposed a realistic (finite size) smooth profile for the dielectric interface. We have found that the excitonic binding energy can either be higher than the corresponding one to complete confinement by infinite barriers or essentially zero for a wide range of dot sizes depending on the thickness of the dielectric interface.

## 1. Introduction

The increasing experimental capabilities in the fabrication of semiconductor nano-crystallites (quantum dots, QD) for a wide spectra of sizes, drives the experimental and theoretical interest for the overall comprehension of these systems since, due to the quantum confinement, the electronic and optical properties are strongly dot size-dependent [1]. In particular, it is well established that the optical band-gap energy is augmented (as compared with bulk values) towards higher energies when the dot size decreases. This behaviour is the result of two opposite effects: while the single-particle band-gap energy is shifted to higher energies, the binding energy of the electron-hole pair (exciton) created by photoexcitation adds an attractive correction which gives rise to a net blue shift but with a weaker dot size-dependence as compared with the corresponding single-particle band-gap energy.

The first and simplest theoretical approach used in the analysis of electronic properties of nanostructures was the effective mass approximation (EMA) [2, 3], which in principle is capable of covering the full range from large to small quantum dots, with the length scale given roughly by a few lattice constants. It is then clear that there should exist a critical dot size for the validity of the EMA, below which the approximation (essentially based in the semiconductor bulk properties) must fail. Fortunately, in this limit of very small crystallites (up to a maximum diameter of about 30 Å) other more microscopic approaches such as the

[1] Permanent address: Facultad de Formación Docente en Ciencias y Facultad de Ingeniería Química, Universidad Nacional del Litoral (UNL), Santiago del Estero 2829, 3000 Santa Fe, Argentina.

0953-8984/01/020319+16$30.00 © 2001 IOP Publishing Ltd Printed in the UK 

empirical tight-binding (ETB) [4–7], the empirical pseudopotential method (EPM) [8–10], and *ab initio* pseudo-potential calculations [11] are possible and improvements in quantitative agreement with experimental results has been reached in this small size regime. Based in a comparison between their results for the single-particle band-gap energy, the Coulomb and exchange excitonic corrections and the corresponding EMA results, some authors of this group [10, 11] conclude by disregarding the EMA as a quantitative, and even qualitative method for the study of nanocrystallites. However, we must pay attention to the fact that in most cases the EMA results were obtained under the assumption of perfect confinement (infinite barriers, IEMA) for both electron and hole. Several authors [12, 13] pointed out that this extreme hard-wall constraint (which is not inherent to this approach) is the main reason for the discrepancy with more microscopic approaches and carried out calculations assuming an incomplete confinement (finite barriers, FEMA) for the electron and hole. The output of such calculations is that while the single-particle band-gap energy is not well described by FEMA, excellent quantitative agreement was obtained for the excitonic properties with the more sophisticated calculations available at present. This can be understood from the fact that while single-particle properties depend directly on the fine structure of the electron and hole envelope functions, exciton properties are given by averaged (integrated) expectation values with these envelope functions (see below). As a consequence, excitonic related properties are much less sensitive to fine details of the electron and hole wave-functions than single-particle properties. The encouraging results obtained in this way allow us to keep FEMA as a qualitative, flexible and versatile theoretical tool for the study of the excitonic physics of quantum dots.

Another question to analyse in detail to make a full comparison between theory and experiment is the change in the excitonic energy due to the dielectric mismatch between the quantum dot and the surrounding matrix. This immediately raises the issue that electrostatic screening in semiconductor quantum dots is expected to be different from its bulk counterpart. In particular, reasonable doubts arise if a macroscopic treatment based on the use of an effective dot dielectric constant ($\varepsilon$) is still meaningful. This topic was recently addressed in three different calculations, a phenomenological one [14], and two full quantum mechanical ones [6, 15]. They conclude that the confinement should reduce $\varepsilon$, although they differed with respect to the magnitude of this reduction. Besides, and this is the key point, in the last two microscopic calculations, through a careful comparison between microscopic and macroscopic results for the electrostatic screening, the validity of macroscopic type treatments was established, although with suitable generalizations.

This size-dependent effect on the dot dielectric response can be easily incorporated to our approach, but we show at the end of section 3 that this correction is quantitatively small compared with the size-dependence effects on the Coulomb and self-energies. Consequently, in the rest of the paper we ascribe to the dot a bulk dielectric constant, which is an excellent approximation for not too small quantum dots (dot diameter, $d \gtrsim 20$ Å). For simplicity, most of the time the effect of the dielectric mismatch is incorporated assuming that the dielectric constant changes discontinuously from its value in the quantum dot to the value corresponding to the matrix (step-like model, see figure 1(a)). In this case, and according to the classical image-charge concepts of basic electrostatics [16], the presence of a charged particle inside the quantum dot induces charges at the boundaries which have the same sign as the source charge if the dielectric constant inside the dot is higher than outside (the general situation). Within IEMA, this gives rise to a repulsive (positive) potential energy corresponding to the particle interacting with its own induced charge; this is usually denoted as a self-polarization energy correction. Besides, when we study excitons, the polarization effects also modify the direct Coulomb interaction since the induced charge by the electron (hole) can attractively interact with the hole (electron) for the usual case. Consequently, there are two opposite contributions

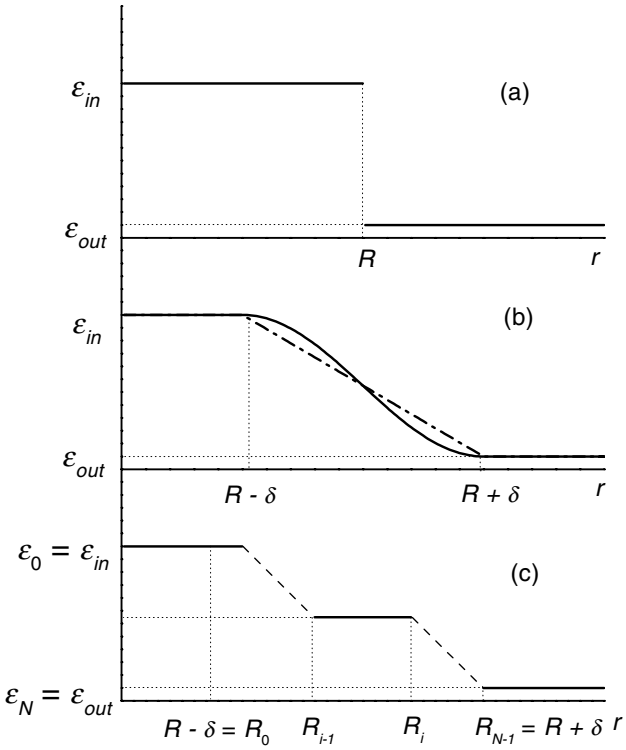


**Figure 1.** Spatial profiles for the dielectric interface. (a) step-like model; (b) linear (dot-dashed line) and cosine-like (full line) models; (c) schematic discretization by $N$-steps of an arbitrary model of the dielectric interface. The step-like model corresponds to the choice $\delta = 0$, $N = 1$, while in the limit $N \to \infty$ the profile of figure 1(c) can be made arbitrarely close to any of the continous profiles of figure 1(b).

to the excitonic energy due to polarization effects. For spherical quantum dots, and assuming (i) infinite confinement for the particles (IEMA) and, (ii) a step-like model for the dielectric profile, it is possible to demonstrate [6] that both effects are almost exactly compensated and then the excitonic energy reduces to the bare electron-hole attraction. In previous work, we have verified that the same cancellation occurs for cubic quantum dots [17]. However, as we show in this work, as soon as we relax these two strong assumptions, the compensation between the polarization effect is no longer fulfilled. Therefore, the two polarization contributions to the exciton energy must be taken into account in a more realistic way.

A direct consequence of the step-like dielectric profile is that all of the induced charge is perfectly localized at the surface boundary, leading to a divergent self-polarization potential at the dot surface. This feature is not compatible with the electron and hole incomplete confinement associated with finite potential barriers, since in this case both the particle and its induced charge could coincide at the dot boundary and then the self-polarization energy diverges[2]. This unphysical result clearly shows that the standard electrostatic description of

[2] For example, for the step-like model of the dielectric interface, the partial-wave expansion of equation (12) diverges as the geometrical series for $r \to R$, but with two different coefficients depending if $\boldsymbol{r}$ approaches $R$ from inside or outside the dot. This means that the potential singularity at the dot surface is not integrable in the sense of a principle value integral; more precisely, it leads to a logarithmic divergence with the sum index $l$ when the sum of equation (12) is attempted for a finite barrier case.

the interface between dielectric media fails at distances comparable to the interatomic distance. The difficulty is automatically solved in the infinite barrier case: as a consequence of the hard-wall boundary condition the electron and hole envelope wave-functions are zero precisely where the self-induced potential diverges (the dot boundary), and then the self-polarization energy remains finite. For the finite barrier case, the anomalous behaviour can be 'regularized' by introducing a phenomenological cut-off distance of the same order of magnitude as the interatomic distance [19–21]. However, this proposal of modifying the functional form of the potential does not follow from any calculation; it is only a mathematical trade-off designed to avoid the divergence. A more rigorous approach was carried out by Stern [21] who, in the study of a semiconductor–insulator $Si/SiO_2$ planar interface, solves the problem by proposing a model dielectric interface in which the dielectric constant changes continuously between its extreme values (see figure 1(b) for our three-dimensional analogue). In this way the induced charge is spread along the dielectric interface region and the divergence in the self-polarization energy disappears, as it physically should be. The consideration of an interface with finite thickness is in parallel with the situation in real samples because the experimental growth procedures do not guarantee a sharp profile without interdiffusion between dot and matrix materials.

As discussed above, the evaluation of the optical band-gap requires two independent calculations: the single-particle band-gap energy (blue shift) and the excitonic corrections (red shift). By using EMA, the accurate calculation of the former contribution requires consideration of other ingredients as a multiband $\boldsymbol{k}\cdot\boldsymbol{p}$ finite barrier calculation of the dot band structure [22], which is beyond the scope of the present work. Therefore, the aim of the present paper is to give insights about the excitonic correction in quantum dots when the combined effects of partial confinement by finite barriers and dielectric mismatch are considered.

The paper is organized as follows: in section 2 we give the basic formulae used for the calculation of the excitonic energies, in section 3 we discuss the results, and finally in section 4 we summarize our conclusions.

## 2. Theory

In previous work [17] we demonstrated that the excitonic properties (even in the presence of a large dielectric mismatch) are essentially independent of the dot shape, so we will concentrate our analysis in the simplest geometry: spherical quantum dots with radius $R$. We attach to the dot-acting semiconductor a dielectric constant $\varepsilon_{in}$, while the outside media where the dot is embedded has a dielectric constant $\varepsilon_{out}$, and we will study the effect of different models for the dielectric interface connecting both limits (see figure 1). Within the envelope wave-function approach to the effective mass approximation [23], the relevant Hamiltonian for an electron-hole system is given by

$$H(\boldsymbol{r}_e, \boldsymbol{r}_h) = H_e(\boldsymbol{r}_e) + H_h(\boldsymbol{r}_h) + V_c(\boldsymbol{r}_e, \boldsymbol{r}_h) \tag{1}$$

where the first and second terms on the right-hand side are the single-particle contributions for the electron and hole respectively, and the last one is the generalized electron-hole Coulomb interaction (to be discussed below). The single-particle Hamiltonian $H_i(\boldsymbol{r}_i)$ $(i = e, h)$ is defined as

$$H_i(\boldsymbol{r}_i) = -\nabla_i \frac{\hbar^2}{2m_i(\boldsymbol{r}_i)}\nabla_i + V_s(\boldsymbol{r}_i) + V_{0i}(\boldsymbol{r}_i) \tag{2}$$

where the first term is the kinetic energy for a particle with effective mass $m_i(\boldsymbol{r}_i)$, $V_s(\boldsymbol{r}_i)$ corresponds to the above discussed self-polarization energy that can be obtained as a particular case of $V_c(\boldsymbol{r}_e, \boldsymbol{r}_h)$ (see below), and the last one is the confining potential which we assume as

a spherical quantum well-like potential defined by $V_{0i}(\boldsymbol{r}_i) \equiv \Theta(r_i - R)\, V_{0i}$, $\Theta$ being the step function and $V_{0i}$ the barrier height. The dependence of $m_i$ on $\boldsymbol{r}_i$ arises from the fact that the particles have different effective masses depending on their location, inside or outside the dot.

### 2.1. Coulomb and self-polarization potentials

The generalized Coulomb potential between two particles with coordinates $\boldsymbol{r}$ and $\boldsymbol{r}'$, and charges $e$ and $e'$ respectively, can be calculated through $V_c(\boldsymbol{r}, \boldsymbol{r}') = e\,\Phi(\boldsymbol{r}, \boldsymbol{r}')$, where $\Phi(\boldsymbol{r}, \boldsymbol{r}')$ is the electrostatic potential which verifies the Poisson equation

$$\nabla_r \cdot \varepsilon(\boldsymbol{r})\, \nabla_r \Phi(\boldsymbol{r}, \boldsymbol{r}') = -4\pi e' \delta(\boldsymbol{r} - \boldsymbol{r}') \tag{3}$$

where $\varepsilon(\boldsymbol{r})$ is the (local) spatially dependent dielectric function. This equation is quite simple to solve analytically if we assume that $\varepsilon(\boldsymbol{r})$ depends only on $r$, and also that the spatial dependence for $\varepsilon(r)$ corresponds to the step-like model, as shown in figure 1(a) (for instance, see Banyai and Koch [1] and [3]). The important points in the derivation of such solutions are: first, under the assumption of a spherical symmetry equation (3) is separable in angular and radial parts, being only the resulting radial differential equation the non-trivial part to solve; second, the solution of this radial equation is easy to find if $\varepsilon(r)$ is constant. For this particular case, the radial solution of equation (3) consists of product of powers of the coordinates $r$ and $r'$; the step-like model of figure 1(a) allows then to propose for each region at both sides of the interface two different solutions of this type, and finally obtains the solution for the whole space through the standard electrostatic boundary conditions which $\Phi$ should satisfy at the interface. It is also possible to obtain an analytical solution of equation (3) in the case where $\varepsilon(\boldsymbol{r})$ depends linearly on only one coordinate, we say $z$, and is independent of $x$ and $y$, as, for example, in the case of a simple semiconductor–insulator junction [21]. The disappointing feature of this exact solution is that the electrostatic potential exhibits a logarithmic divergence at the edges of the transition layer, which can be traced back to the discontinuous first derivative at these points of the linear model for the dielectric interface. The three-dimensional solution for the linear model of the dielectric interface, even assuming spherical symmetry, is quite complicated to find since equation (3) becomes a second-order differential equation with spatially dependent coefficients. We will not pursue the analytical resolution of this problem, which even if feasible, is restricted to just a particular model for the dielectric interface.

Instead, by exploiting the exact solution of the single-step case, and following the spirit of [22], we will consider an *arbitrary* smooth radial profile for $\varepsilon(r)$ and proceed as follows: first we define a finite interface of width $2\delta$ centred at $R$. For $r < R - \delta$ (well inside the dot) the dielectric constant takes the value corresponding to the bulk dot-acting semiconductor, $\varepsilon(r) \equiv \varepsilon_{in}$. For $r > R + \delta$ (well outside the dot), $\varepsilon(r)$ is fixed at the value corresponding to the surrounding matrix, $\varepsilon(r) \equiv \varepsilon_{out}$. Between them, for $R - \delta < r < R + \delta$, we can choose any analytical and physically plausible function that connects these extreme values (as pictured in figure 1(b)). Afterwards, we subdivide the dielectric interface in $N - 1$ regions and in each one of them we approximate the dielectric function by a constant value (typically the mean value of the selected function in this zone). Thus, the original continuous profile is approximated by an $N$-step one in which each single-step problem has a known solution. This approach allows us to connect $\varepsilon_{in}$ and $\varepsilon_{out}$ with any arbitrary function being the number of steps $N$ the only parameter to adjust, the condition being that it should provide a good approximation to the true connecting function. Strictly, our approach is such that when $N \to \infty$ we recover the exact solution of equation (3). As a result of this procedure, the expression for the generalized

Coulomb potential is (see figure 1(c) to clarify the notation)

$$V_c^{i,m}\left(\boldsymbol{r},\boldsymbol{r}'\right)=\frac{ee'}{\varepsilon_m}\sum_{l=0}^{\infty}P_l\left(\cos\gamma\right)\frac{F_{im,l}\left(r,r'\right)}{\left(1-p_{m,l}q_{m,l}\right)} \tag{4}$$

where the superindex $i$ ( $m$ ) indicates that the particle with coordinate $\boldsymbol{r}$ ( $\boldsymbol{r}'$ ) is placed at the $i$-region ($m$- region); $P_l\left(\cos\gamma\right)$ are the Legendre polynomials of order $l$ and $\gamma$ is the angle between both particles (measured from the origin at the dot centre). With $i$ and $m$ taking values between 0 and $N$, the Coulomb potential $V_c(\boldsymbol{r},\boldsymbol{r}')$ is defined in the whole space. The functions $F_{im,l}\left(r,r'\right)$ are given by

$$F_{im,l}\left(r,r'\right)=\left[p_{m,l}r_>^l+r_>^{-(l+1)}\right]\left[r_<^l+q_{i,l}r_<^{-(l+1)}\right]\prod_{j=i}^{m-1}\frac{1+q_{j+1,l}R_j^{-(2l+1)}}{1+q_{j,l}R_j^{-(2l+1)}} \tag{5}$$

if $i<m$,

$$F_{im,l}\left(r,r'\right)=\left[p_{m,l}r_>^l+r_>^{-(l+1)}\right]\left[r_<^l+q_{m,l}r_<^{-(l+1)}\right] \tag{6}$$

for $i=m$ and

$$F_{im,l}\left(r,r'\right)=\left[p_{i,l}r_>^l+r_>^{-(l+1)}\right]\left[r_<^l+q_{m,l}r_<^{-(l+1)}\right]\prod_{j=m+1}^{i}\frac{1+p_{j-1,l}R_{j-1}^{2l+1}}{1+p_{j,l}R_{j-1}^{2l+1}} \tag{7}$$

when $i>m$. In the previous equations $r_<$ ($r_>$) is the smallest (greatest) distance between $r$ and $r'$. The $q_{i,l}$ coefficients are defined so that $q_{0,l}=0\,(\forall l)$ and for $0<i\leqslant m$ are expressed through the following recursive expressions

$$q_{i,l}=\frac{S_{21}^{i,l}+q_{i-1,l}S_{22}^{i,l}}{S_{11}^{i,l}+q_{i-1,l}S_{12}^{i,l}} \tag{8}$$

where the $\boldsymbol{S}$-matrix is

$$\boldsymbol{S}^{i,l}=\begin{bmatrix}\varepsilon_i\,(l+1)+\varepsilon_{i-1}l & (l+1)\,(\varepsilon_i-\varepsilon_{i-1})\,R_{i-1}^{-(2l+1)}\\ l\,(\varepsilon_i-\varepsilon_{i-1})\,R_{i-1}^{2l+1} & \varepsilon_i l+\varepsilon_{i-1}\,(l+1)\end{bmatrix}. \tag{9}$$

Similarly for the $p_{i,l}$ coefficients, $p_{N,l}=0\,(\forall l)$ and for $m\leqslant i<N$

$$p_{i,l}=\frac{p_{i+1,l}E_{11}^{i,l}+E_{12}^{i,l}}{p_{i+1,l}E_{21}^{i,l}+E_{22}^{i,l}} \tag{10}$$

where the $\boldsymbol{E}$-matrix is

$$\boldsymbol{E}^{i,l}=\begin{bmatrix}\varepsilon_i\,(l+1)+\varepsilon_{i+1}l & (l+1)\,(\varepsilon_i-\varepsilon_{i+1})\,R_i^{-(2l+1)}\\ l\,(\varepsilon_i-\varepsilon_{i+1})\,R_i^{2l+1} & \varepsilon_{i+1}\,(l+1)+\varepsilon_i l\end{bmatrix}. \tag{11}$$

Some interesting features of equations (4)–(11) are: (i) the coefficients $q_{i,l}$ and $p_{m,l}$ are all identically zero in the absence of a dielectric mismatch at the dot boundary ($\varepsilon_{in}=\varepsilon_{out}$); (ii) the function $F_{im,l}(r,r')$ defined in equations (5)–(7) has four different contributions, corresponding to particle–particle interactions (the term $r_<^l\,/\,r_>^{l+1}$), particle-induced charge interactions (the two terms either proportional to $q_{i,l}$ or $p_{m,l}$), and the induced charge–induced charge interaction (the term proportional to the product $q_{i,l}\;p_{m,l}$). Only the first one, which represents the bare Coulomb interaction, survives in the homogeneous limit $\varepsilon_{in}=\varepsilon_{out}$; (iii) in the calculation of $V_c^{i,m}(\boldsymbol{r},\boldsymbol{r}')$, only the $q_{i,l}$'s ($p_{m,l}$'s) with $0<i\leqslant m$ ($m\leqslant i<N$) are necessary. For the exciton problem, $e'=-e$.

From equations (4) and (6), the self-polarization potential can be calculated by taking $r=r'$, $e=e'$, eliminating from (6) the direct contribution $r_<^l\,/\,r_>^{l+1}$, and dividing by 2 as corresponds to a self-energy. The result is

$$V_s^m\left(\boldsymbol{r}\right)=\frac{e^2}{2\varepsilon_m}\sum_{l=0}^{\infty}\frac{1}{\left(1-p_{m,l}q_{m,l}\right)}\left[p_{m,l}r^{2l}+p_{m,l}q_{m,l}r^{-1}+q_{m,l}r^{-2(l+1)}\right]. \tag{12}$$

With $m$ running from 0 to $N$, the self-polarization potential $V_s(\boldsymbol{r})$ is defined in the whole space.

It is straightforward to check that in the limit of $\delta = 0$ ($N = 1$), equations (4) and (12) reduced to the usual expressions for $V_c$ and $V_s$ used in the study of spherical QD's with a boundary dielectric mismatch [3, 6, 24].

The choice of different profiles for the dielectric interface modify both the strength and the functional form of the potentials. In figure 2 we show the self-polarization potential (figure 2(a)) and the $l = 0$ component of the generalized Coulomb potential[3] (figure 2(b)) for a small quantum dot where $R = 10$ Å, $\varepsilon_{in} = 12.6$ (GaAs), $\varepsilon_{out} = 1$ (vacuum). The dot-dashed curves correspond to the case of the step-like model for $\varepsilon(r)$ (that is $\delta = 0$ and $N = 1$). The self-polarization potential for this case exhibits the already discussed divergent behaviour at the interface, which leads to a divergent self-energy for the finite barrier situation. The dotted curve is the result of choosing a linear model for the dielectric interface between $\varepsilon_{in}$ and $\varepsilon_{out}$, and the solid line corresponds to a profile proportional to a cosine function; in both cases, $\delta = 5$ Å and $N = 500$. We can observe in figure 2(a) that the consideration of a finite interface (independently of the form of $\varepsilon(r)$) eliminates the divergence present when $\delta = 0$. It is worth emphasizing here the important difference between the 'regularized' self-polarization potential and the solutions which arise from the finite size dielectric interface. Faced with the dilemma of a divergent self-polarization potential and accordingly a divergent self-energy, no physical guidance (except that the final result should be finite) helps one in choosing a regularization procedure for the step-like model of the dielectric interface. In our approach, we do have such a physical guidance: the dielectric function must change smoothly in moving from the dot towards the matrix (presumably on the scale of a few Å), and from this physically plausible assumption the non-divergent self-polarization potential emerges naturally from the calculation. The lack of physical guidance for the case of a step-like model of the dielectric interface is clearly reflected in the fact that the 'regularized' self-polarization potentials of previous works [19–21] are quite different from our physically correct self-polarization potentials shown in figure 2. For instance, a regularized potential following the criteria of [21] amounts to replace the dot-dashed curve for 5 Å$< r <$ 15 Å by a straight line connecting the black dots.

Similar to the planar semiconductor-insulator interface, the linear model for the dielectric interface leads to a potential which exhibits singular points at the left and right edge of the interface[4], precisely where the derivative of $\varepsilon(r)$ is not continuous. While from our numerical approach it is difficult to determine the type of singularity, it can be easily integrated numerically, so we can safely state that the singularity is integrable. However, a cosine-like function seems to be a more physical choice because it gives rise to a well-defined self-polarization potential everywhere. An important feature of this potential for all cases is that it can be either repulsive or attractive. When the source charge is located in the region with greater dielectric constant, the induced charge has the same sign as the source and then the interaction is repulsive. On the contrary, if the source charge is placed in the zone with a lower dielectric constant, the induced charge has an opposite sign and the interaction is attractive. Note, however, the strong asymmetry between the repulsive and attractive potential strengths. In the next section, we will see that this singular behaviour has a relevant role on the calculation of the excitonic energies.

[3] This is the only component that enters in the calculation of the Coulomb energy for the ground-state exciton; on the contrary, all the infinite $l$ components should be kept in the calculation of the self-polarization energy. In practice, when the sum converges, it is truncated after $l$ and reaches a value such that the result remains constant.

[4] The left kink of the linear model for the dielectric interface is not discernible in the scale of the drawing of figure 2(a).

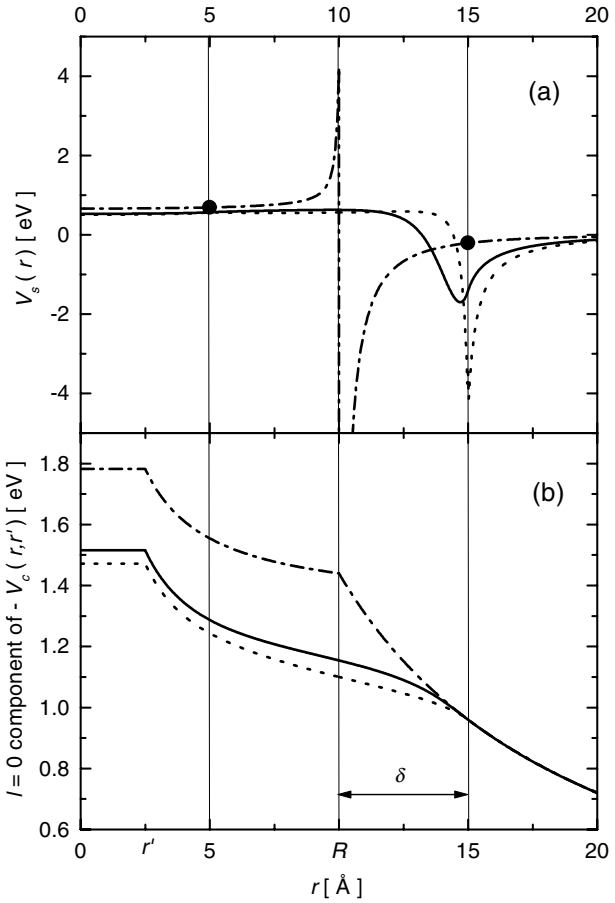


**Figure 2.** Self-polarization potential (a), and $l = 0$ component of the generalized Coulomb potential (b) as a function of $\boldsymbol{r}$, for a quantum dot with $R = 10$ Å, and several models of the dielectric interface. Dot-dashed line, $\delta = 0$; dotted line, $\delta = 5$ Å (linear profile); solid line, $\delta = 5$ Å (cosine-like profile). For the generalized Coulomb potential, the source charge is located at $r' = 2.5$ Å.

Regarding the generalized Coulomb potential $V_c$, all the curves have the universal expected $r^{-1}$ decay screened by $\varepsilon_{out}$ outside the dot ($r > R + \delta$) . The results for linear- or cosine-like profiles for $\varepsilon\,(r)$ are very similar (dotted and solid lines, respectively), the potential strength in both cases being smaller compared with the step-like model. This can be explained as follows; from equation (4), the $l = 0$ component of the generalized Coulomb potential for the step-like model for the dielectric interface is

$$V_c^{0,0}(\boldsymbol{r}, \boldsymbol{r}') = -\frac{e^2}{\varepsilon_{in} R}\left(\frac{R}{r'} + \frac{\varepsilon_{in} - \varepsilon_{out}}{\varepsilon_{out}}\right) \tag{13}$$

for $r < r'$ (the region where the potential is constant of figure 2(b)). The first term in equation (13) corresponds to the bare Coulomb potential, the second to the potential generated by the charges induced at the dot boundary. Note that this term is proportional to the difference of dielectric constants at both sides of the interface; consequently, by giving a finite size to the dielectric interface this term can only decrease in magnitude, as the difference between two successive dielectric constants approach zero for $N \to \infty$. Already from the results presented

in figure 2(b) a decrease of the Coulomb energy of the exciton for the case of a finite size dielectric interface can be anticipated, as compared with the $\delta = 0$ interface.

### 2.2. Zero-order eigenvalues and eigenfunctions

As we consider quantum dots with characteristic dimensions smaller than the exciton effective Bohr radius, we will use the strong confinement approximation (SCA) for the calculation of the eigenvalues, wave-functions, and excitonic energies [2, 3]. In this approach the self-polarization and Coulomb interactions (which scales as $R^{-1}$) are considered as a perturbation against the kinetic energy (which scales as $R^{-2}$). According to this, we propose a separable wave-function for the electron-hole system $\Psi(\boldsymbol{r}_e, \boldsymbol{r}_h) \cong \psi_e(\boldsymbol{r}_e)\psi_h(\boldsymbol{r}_h) = R_{nl}(r_e) Y_{lm}(\theta_e, \varphi_e) R_{n'l'}(r_h) Y_{l'm'}(\theta_h, \varphi_h)$, where $R_{nl}(r_i)$ are the radial component of the wave-function, and $Y_{lm}(\theta, \varphi)$ are spherical harmonics. As a consequence, the resolution of the zero-order Hamiltonian consists of two equivalent problems

$$H_i^{(0)}(\boldsymbol{r}_i)\psi_i(\boldsymbol{r}_i) = \left[-\nabla_i \frac{\hbar^2}{2m_i(\boldsymbol{r}_i)}\nabla_i + V_{0i}(\boldsymbol{r}_i)\right]\psi_i(\boldsymbol{r}_i) = E_i\psi_i(\boldsymbol{r}_i) \tag{14}$$

where $i = e, h$.

The complete solutions of equation (14) turned out to be spherical Bessel functions of real and imaginary arguments [25]; focusing the attention on the ground-state ($n = 1, l = m = 0$), the angular contribution of $\psi_i(\boldsymbol{r}_i)$ becomes a constant and the normalized solution of equation (14) is

$$\psi_i(\boldsymbol{r}_i) = \frac{A_i}{\sqrt{4\pi}}\left[\Theta(R - r_i)\frac{\sin\left(k_i^{in} r_i\right)}{r_i} + \Theta(r_i - R) B_i \frac{\exp\left(-k_i^{out} r_i\right)}{r_i}\right] \tag{15}$$

where the eigenvalues are defined through $k_i^{in} = (2m_i^{in} E_i/\hbar^2)^{1/2}$ and $k_i^{out} = \left[2m_i^{out}(V_{0i} - E_i)/\hbar^2\right]^{1/2}$. As the electron (or hole) has a different effective mass depending on the material, the wave-function must verify the Ben Daniel–Duke boundary conditions [23], i.e. $\psi_i\left(R^-\right) = \psi_i(R^+)$ and $\psi_i'\left(R^-\right)/m_i^{in} = \psi_i'(R^+)/m_i^{out}$. By applying this special boundary condition we arrive at the following implicit eigenvalue equation for the quantum dot energies

$$k_i^{in} R \cot\left(k_i^{in} R\right) = 1 - \frac{m_i^{in}}{m_i^{out}}\left(1 + k_i^{out} R\right). \tag{16}$$

$A_i$ and $B_i$ are constants determined by normalization requirements and are equal to $A_i = \left[R/2 - \sin\left(2k_i^{in} R\right)/4k_i^{in} + \sin^2\left(k_i^{in} R\right)/2k_i^{out}\right]^{-1/2}$ and $B_i = \exp\left(k_i^{out} R\right)\sin\left(k_i^{in} R\right)$.

An important point in this treatment is that we maintain a sharp-profile (step-like model) for the electronic interface, choosing its boundary at the midpoint of the dielectric interface; a more rigorous treatment should also give a finite size to the electronic interface. Our approximation is justified for not too small QD's, as the electronic interface is a small fraction of the total dot size, and accordingly zero-order eigenvalues and wave-functions are weakly dependent on the finite size of the interface (typically a few ångströms).

In order to quantitatively support this approximation for the electronic interface, we present in figure 3 a calculation of the first-order correction to the square-well eigenvalues, when the confining potential is modified in correspondence with the finite size of the dielectric interface. In particular, we adopt the same cosine-like profile for the finite-size electronic interface as for the finite-size dielectric interface. Accordingly, full, dashed-dotted, and dotted lines correspond to the cosine-like electronic interface with $\delta = 0$, 2 and 5 Å. In the last two cases, the eigenvalues were obtained treating as a perturbation the difference between the cosine- and step-like electronic profiles. In the worse case of $\delta = 5$ Å, the correction amounts to about

10 %, while for $\delta = 2$ Å (not shown) is much smaller ($\sim 3$ %). Similar differences could be expected for the perturbed wave-functions. It is interesting to note that as the perturbed eigenvalue is above the corresponding step-like electronic profile, one can also expect a greater penetration in the barrier. However, the decay of the perturbed wave function starts before the decay of the unperturbed one, and consequently some compensation exists between both effects. Finally, the example displayed in figure 3, with $\delta/R = 0.5$ (for $\delta = 5$ Å) can be considered as the less favourable configuration for this approximation, as the error decreases with $\delta/R$. For instance, for $\delta/R = 5$ Å / 20 Å $= 0.25$, the difference between perturbed and unperturbed eigenvalues is only about 5%.

### *2.3. Exciton Coulomb energy*

The exciton Coulomb energy is defined as the correction to the single-particle size-dependent band-gap energy needed to create an electron-hole pair inside the quantum dot. Then, this excitonic energy includes the generalized Coulomb interaction between the negative and positive charges as well as the self-polarization energies corresponding to the electron and the hole,

$$E_{ex} \equiv \Sigma_e + \Sigma_h - E_{Coul}. \tag{17}$$

The Coulomb energy $E_{Coul}$ and the self-polarization ones, $\Sigma_e$ and $\Sigma_h$, are calculated within the SCA by performing the average value of $V_c$ and $V_s$ (equations (4) and (12), respectively) using the zero-order wave-functions given by (15) in [17]

$$\Sigma_i \equiv \int \mathrm{d}\boldsymbol{r}_i \psi_i^* (\boldsymbol{r}_i)\, V_s (\boldsymbol{r}_i)\, \psi_i (\boldsymbol{r}_i) \tag{18}$$

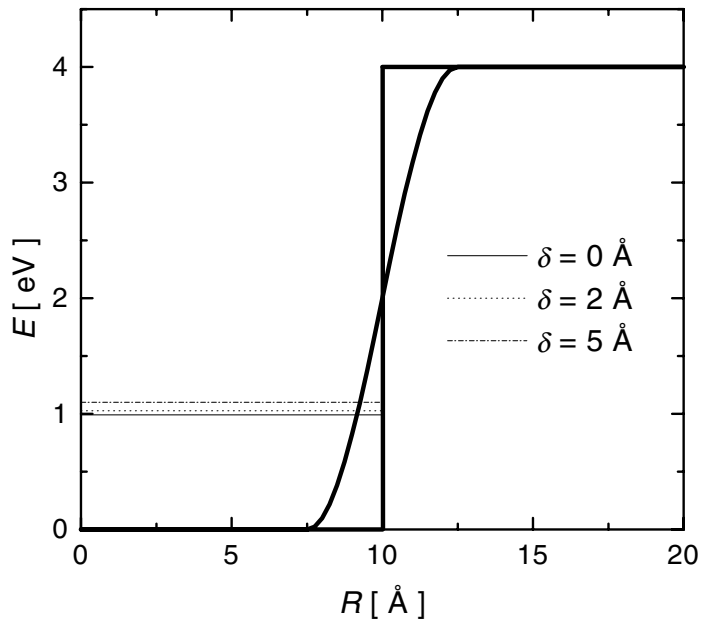


**Figure 3.** Bound-state eigenvalues (thin lines) of the quantum dot spherical well, for the step- and cosine-like models (thick lines) of the electronic interface. For $\delta = 0$ ($\delta \neq 0$) the eigenvalues are exact (approximated), as explained in the text. For this particular dot size, only one bound-state exists in the spherical well.

$$E_{Coul} \equiv -\int \mathrm{d}\boldsymbol{r}_e \mathrm{d}\boldsymbol{r}_h \, |\psi_e(\boldsymbol{r}_e)|^2 \, V_c(\boldsymbol{r}_e, \boldsymbol{r}_h) \, |\psi_h(\boldsymbol{r}_h)|^2 . \tag{19}$$

Defined in this way, $E_{Coul}$ for the electron-hole pair is always positive. For the finite barrier case, $\Sigma_i$ can be either positive or negative, while for the infinite barrier case $\Sigma_i$ is always positive.

## 3. Results

The results of this section were obtained using the material parameters summarized in table 1, corresponding to a GaAs QD immersed in a vacuum. We chose this system for several reasons: (i) the choice of vacuum as the surrounding media considerably simplifies the material parameter choice, as $V_{0e}$ is given by the electron affinity of the semiconductor dot material in bulk, while for our simple two-band semiconductor model, $V_{0h} \to \infty$; (ii) the high-dielectric mismatch between GaAs and vacuum maximize the effect of the induced charge at the dot boundary in which we are interested. An important point to make is that all of the constants characterizing the materials were extracted from the bulk values and consequently they are not adjustable parameters. Also, all of the results to be presented below for the self-polarization, Coulomb, and excitonic energies were obtained by using the cosine-like model for the dielectric interface; very similar results were obtained for the linear model of the dielectric interface.

Figure 4(b) shows the results for the Coulomb energy (equation (19)), for several sizes of the dielectric interface, as a function of the reciprocal dot diameter $1/d$ ($d = 2R$). As a reference we include a thick curve corresponding to the usually quoted result $E_{Coul}(d) \simeq 3.786\, e^2/d\varepsilon_{in}$ [3] which results from the combination of infinite barriers ($V_{0e} \to \infty$) with a step-like model for the dielectric interface. We can observe that, as was expected from the behaviour of $l = 0$ component of $V_c$ shown in figure 2(b), this contribution to the exciton energy decreases monotonously when the thickness of the dielectric interface increases. The thin line corresponds to $\delta = 0.05$ Å which can be taken as a very good approximation to the $\delta = 0$ case. As was established in [13], as soon as we depart from the infinite barrier approximation, the widely criticized $d^{-1}$ scaling of IEMA is lost. Here, we have demonstrated that it is possible to increasingly modify the size dependence if we consider a finite size dielectric interface connecting the QD material and the surroundings. For instance, for $\delta = 5$ Å the scaling of $E_{Coul}$ with dot size is proportional to $d^{-0.86}$.

The exciton self-polarization energy given by $\Sigma_e + \Sigma_h$ plotted in figure 4(a) shows an interesting behaviour with a non-monotonic dependence on the dielectric interface size. As in figure 4(b), the full thick line corresponds to the infinite barrier limit combined with the step-like model of the dielectric interface; accordingly, the difference between the full thick line ($\delta = 0$, $V_{0e} \to \infty$) and the full thin line ($\delta = 0.05$ Å, $V_{0e} = 4$ eV) is due to the effect of the finite barrier size for the latter. In particular, polarization effects are strongly suppressed for near zero-width interfaces, afterwards these effects are augmented up to $\delta = 2$ Å, but for wider interfaces the self-polarization energy decays again. This singular feature can be understood if we remember that the self-polarization energies are actually the product (integrated over the whole space) between the self-polarization potential $V_s$ and the electron (hole) probability density given by $|r\psi_e|^2$ $\left(|r\psi_h|^2\right)$ (equation (18)). To help with this explanation we present figure 5 where $|r\psi_e|^2$ and $V_s$ are plotted separately. As can be immediately grasped from this figure, the maximum value for the self-polarization energy correction for the combination of total confinement and step-like dielectric interface is a consequence of the fact that the wave-function is different from zero precisely in the same region where the self-polarization potential is positive (inside the dot). The situation changes drastically by relaxing the hard-wall boundary condition, as $|r\psi_e|^2$ spreads considerably outside the dot, where the self-polarization potential is negative.

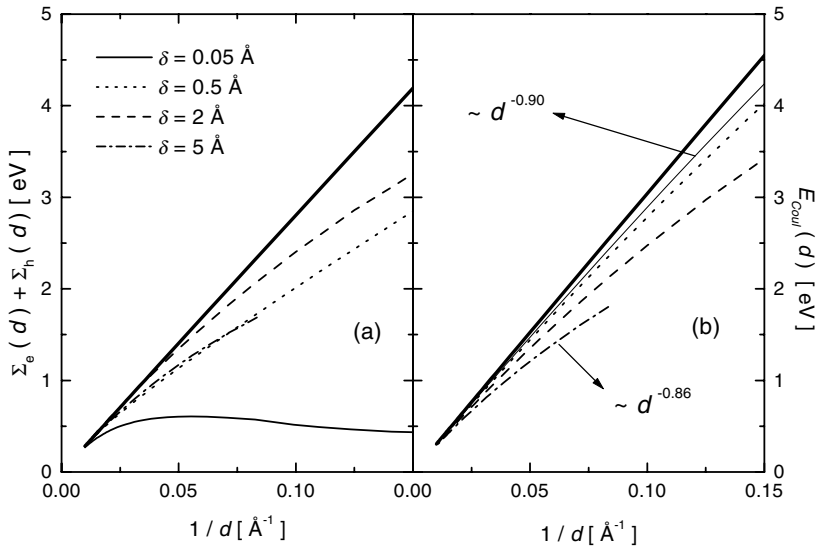


**Figure 4.** Exciton self-polarization energies (a) and Coulomb energies (b) as a function of dot size, for $\delta = 0.05$, 0.5, 2 and 5 Å. The full thick line corresponds to the infinite barrier limit for electrons (and $\delta = 0$), and the remaining curves are for $V_{0e} = 4$ eV.

This explains the strong decrease of $\Sigma_e + \Sigma_h$ by going from $V_{0e} \to \infty$ to $V_{0e} = 4$ eV; actually, as $\Sigma_h$ is always positive (the holes are perfectly confined in the present case) an almost zero value of $\Sigma_e + \Sigma_h$ implies a negative value for $\Sigma_e$. As the dielectric interface increases in size, the negative part of the self-polarization potential moves apart from the electronic interface, $\Sigma_e$ becomes less negative, and $\Sigma_e + \Sigma_h$ increases. Finally, for $\delta \gtrsim 3$ Å, only the positive component of $V_s$ contributes to $\Sigma_e$, and because its value decreases as $\delta$ increases, $\Sigma_e$ shows a non-monotonic behaviour. A final remark about figure 4 is that both $E_{Coul}$ and $\Sigma_e + \Sigma_h$ values never exceed those achieved with the total confinement approximation, which seems to be a kind of upper limit.

Concerning the excitonic energy, the results seem to be less predictable. In figure 6 we show the exciton energies $E_{ex}(d)$ as a function of dot sizes, for quantum dots with $\delta = 0.05$, 0.5, 2, and 5 Å; the IEMA results for $\delta = 0$ are also plotted (thick full line). Contrary to $E_{Coul}$ and $\Sigma_e + \Sigma_h$, much higher excitonic energies than those resulting from IEMA can be reached for QD's with thin interfaces. The explanation for this is clear from the results presented in figure 4: while the self-polarization energy decreases strongly by going from $V_{0e} \to \infty$ to $V_{0e} = 4$ eV, the Coulomb energy remains essentially unaltered under such changes in confinement. Accordingly, the exciton energy, which is the difference between these two magnitudes, increases and becomes similar in magnitude to the Coulomb contribution (roughly, $E_{ex} \sim E_{Coul} / 2$). As the dielectric interface increases in size, the self-polarization energy first increases up to a critical $\delta$, and then decreases: this non-monotonic behaviour of $\Sigma_e + \Sigma_h$ is followed by a non-monotonic behaviour for the exciton energy displayed in figure 6. It is interesting to note that for dielectric interface sizes of about a lattice parameter (2 Å $\lesssim \delta \lesssim$ 5 Å), the excitonic energy correction is very small for all $d \gtrsim 20$ Å. Under these conditions, a measure of the optical band-gap should be compared directly with the single-particle band-gap, without excitonic corrections.

It is worth noting the variety of behaviours that can be obtained for the dot-size dependence

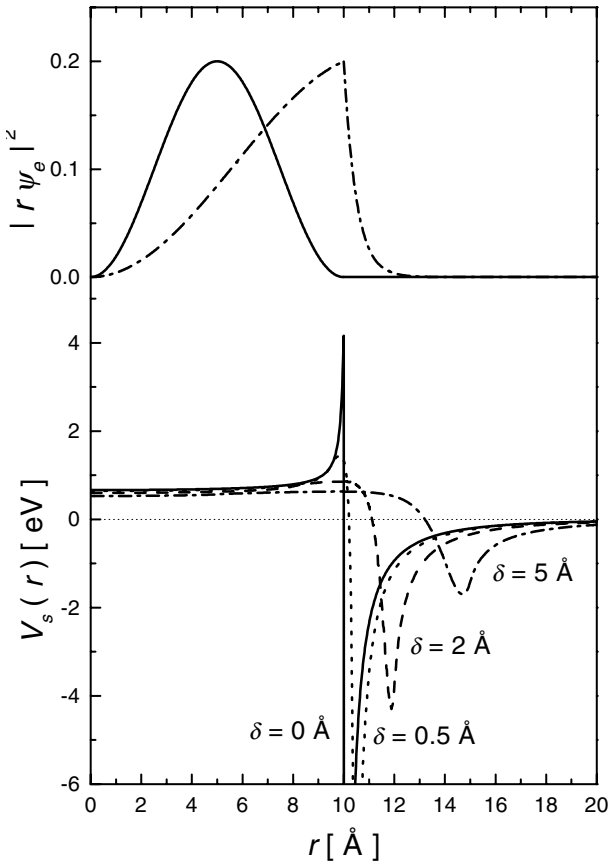


**Figure 5.** Upper panel: probability density associated with the normalized ground-state electronic wave-function, and effective mass mismatch $m_{in}/m_{out} = 0.067$. Full line, $V_{0e} \to \infty$; dashed-dotted line, $V_{0e} = 4$ eV. Lower panel: self-polarization potential for $\delta = 0$, 0.5, 2, 5 Å dot radius, $R = 10$ Å.

of the exciton energy by the combination of partial confinement with a finite size for the dielectric interface. This should be kept in mind when correcting single-particle band-gaps with the excitonic contribution, in order to be able to compare with optical experiments, as this is usually done by using the infinite barrier and step-like model for the dot-confined exciton (full thick line of figure 6).

Before we conclude, let us reasses the issue of the electrostatic screening in semiconductor quantum dots, discussing it in the light of the preceeding results. Firstly, we can easily include in our calculations a size-dependent dielectric constant for the dot. According to the generalized Penn model [14],

$$\varepsilon_{in}(d) = 1 + \frac{\varepsilon_{in} - 1}{1 + (2\alpha/d)^l} \tag{20}$$

with $\varepsilon_{in}$ being the infinite dot size (bulk) dielectric constant, $\alpha = 2\pi E_F/E_g k_F$, and $l = 2$. $E_g$ is taken as the optical gap of the dot-acting semiconductor, and $k_F$ and $E_F$ are determined from the density of valence electrons $n_0$. For GaAs, taking $E_g = 5.2$ eV [26], and $n_0 = 0.1774/\text{Å}^3$, we obtain $\alpha = 8.01$ Å. Inserting this size-dependent dielectric constant in our calculations, we

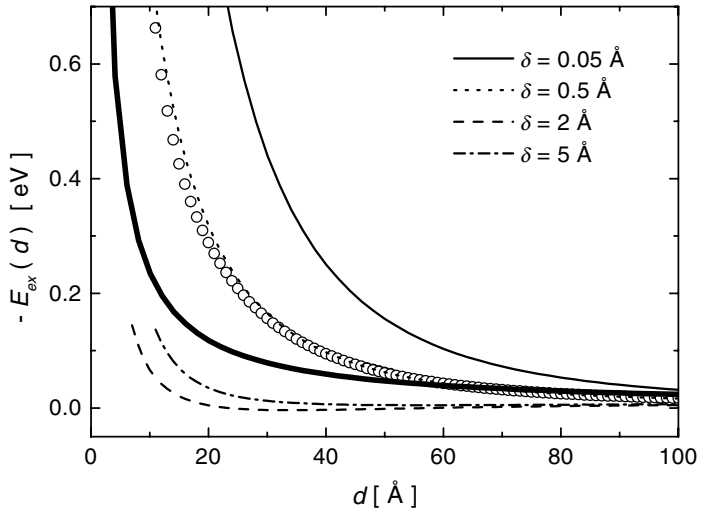


**Figure 6.** Exciton energies as a function of dot size for $\delta = 0.05$, 0.5, 2, and 5 Å. The full thick line corresponds to the infinite barrier limit for electrons (and $\delta = 0$), and the remaining lines are for a barrier of 4 eV. As explained in the text, the curve with open points correspond to the exciton energy obtained by replacing $\varepsilon_{in} = 12.6$ by $\varepsilon_{in}(d)$ as defined by equation (20).

obtain the curve with open points of figure 6 (corresponding to $\delta = 0.5$ Å). It can be seen that this size effect, *although it exists*, is very small for dots with $d \gtrsim 10$ Å.

The related issue of the incomplete screening at short distances in small semiconductor clusters can be discussed along a similar line of reasoning. Generalizing equation (20) as

$$\frac{1}{\varepsilon_{in}(r,d)} = \frac{1}{\varepsilon_{in}(d)} + \left(1 - \frac{1}{\varepsilon_{in}(d)}\right) e^{-r/a} \tag{21}$$

where $\varepsilon_{in}(d)$ is given by equation (20), and $a$ is a screening parameter. For $d \to \infty$, and $\varepsilon_{in}(\infty)$ corresponding to the bulk dielectric constant, the spatially dependent dielectric function of equation (21) is that proposed by Hermanson [27]. The screening parameter $a$ can be obtained from the criteria that the Fourier transform of equation (21) fits the dielectric function of Walter and Cohen [28]. Following Oliveira and Falicov [29], we took $a \simeq 0.58$ Å as the characteristic value for GaAs. Without any calculation, we can argue against the importance of this effect due to the following facts: (i) the spatially dependent screening, as defined by equation (21), for a given dot size is extremely short-ranged, with a typical length scale of about an *atomic* Bohr radius, and (ii) according to equation (20), $\varepsilon_{in}(d \to 0) \to 1$, and then *the correction given by the second term in equation (21) is smaller for smaller dots*. In other words, in this limit $\varepsilon_{in}(r, d \to 0) \to \varepsilon_{in}(d \to 0)$, and the incomplete short-range screening reduces to the size-dependent dielectric function. Let us estimate quantitatively the importance of the second term in equation (21) on the ground-state binding energy of unconfined (bulk) excitons: using first-order perturbation theory the correction (in units of the bulk exciton binding energy $R_0^*$) is given by

$$\frac{\Delta E}{R_0^*} = \frac{8\,[\varepsilon_{in} - 1]}{\left(2 + a_0^*/a\right)^2}, \tag{22}$$

with $R_0^* = e^2/2\varepsilon_{in}a_0^*$, $a_0^* = \hbar^2\varepsilon_{in}/e^2\mu$, and $\mu = m_e m_h/(m_e + m_h)$. Inserting in equation (22) the GaAs parameters of table 1, we obtain $\Delta E/R_0^* \simeq 10^{-3}$. Having discarded the importance

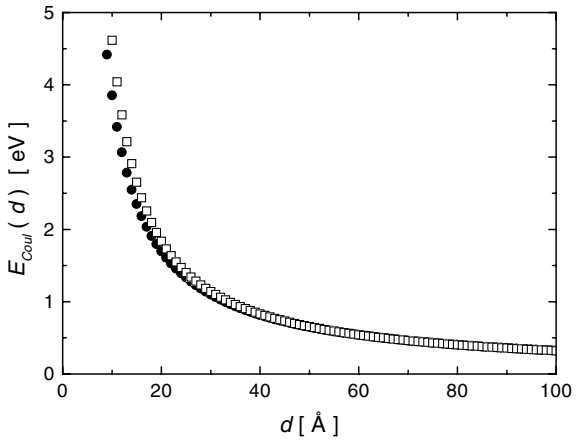


**Figure 7.** Ground-state binding energy of an on-centre donor impurity. Full circles were obtained by using only the first term in the right side of equation (21) and open squares correspond to the results which consider the dielectric function defined by equation (21).

of an incomplete short-range screening for the bulk, let us estimate its relevance for quantum dots. To this end, we have calculated this correction for the case of the ground-state binding energy of an on-centre donor impurity. This could be considered as the limiting case of $m_h/m_0 \gg 1$, as in this case the exciton and the donor impurity problems are equivalent. In order to simplify matters, we take here the infinite barrier approximation. The results are given in figure 7. Here, the circles correspond to use in the calculation of $E_{Coul}(d)$ for the donor impurity using only the first term in the right-hand side of equation(21), while the squares are the results using equation(21) as it is. Once again, short-range effects are found for very small for dot sizes $d \gtrsim 20$ Å.

## 4. Conclusions

In this work we have studied the dependence of Coulomb, self-polarization, and excitonic energies of spherical semiconductor quantum dots with partial confinement on dot size and in the presence of a smooth dielectric interface at the dot boundary. We have developed a numerical method which allows the study of the electrostatic properties of finite-size dielectric interfaces of arbitrary shape; essentially, it consists of replacing the continuous profile of the dielectric interface by a series of discrete steps. In the limit of a very large number of steps (several hundreds), our method provides the exact solution to the electrostatic problem of a graded three-dimensional dielectric interface. The motivation for this analysis is twofold: from the mathematical point of view, the combination finite barrier plus step-like model for the dielectric interface is ill-behaved, as the self-energy of the partially confined particle (electron, hole, or both) diverges in this situation. From the physical point of view, the interface between two semiconductors (or between semiconductor and vacuum) is never perfectly sharp as the step-like model of the dielectric interface assumes. The finite size of the interface becomes a crucial feature for a sensible calculation of the self-energy, although is not so relevant for the Coulomb energy.

We have studied the excitonic energy for linear and cosine-like spatial profiles for the dielectric interface, and for different values of the interface width. Interestingly, the excitonic

energy shows a pronounced and non-monotonic dependence on the interface width, becoming very small for intermediate dielectric interfaces, but becoming quite sizeable for narrow dielectric interfaces. Our results highlight the importance of considering the finite size of the dielectric interface, as quite a variety of excitonic corrections can be obtained depending on the combination barrier height–interface width.

## Acknowledgments

P G B wishes to acknowledge the financial support received from FOMEC 331, Universidad Nacional del Litoral. The authors are grateful to Karen Hallberg for a careful reading of the manuscript.

## References

[1] Yoffe A D 1993 *Adv. Phys.* **42** 173
Banyai L and Koch S W 1993 *Semiconductor Quantum Dots* (Singapore: World Scientific)
Woggon U and Gaponenko S V 1995 *Phys. Stat. Sol.* b **189** 285
1998 *MRS Bulletin special issue Semiconductor Quantum Dots* ed A Zunger **23** (2)
[2] Efros Al L and Efros A L 1982 *Soviet Phys. Semicond.* **16** 772
[3] Brus L E 1983 *J. Chem. Phys.* **79** 5566
Brus L E 1984 *J. Chem. Phys.* **80** 4403
[4] Lippens P E and Lanoo M 1989 *Phys. Rev.* B **39** 10935
[5] Proot J P, Delerue C and Allan G 1992 *Appl. Phys. Lett.* **61** 1948
[6] Lannoo M, Delerue C and Allan G 1995 *Phys. Rev. Lett.* **74** 3415
[7] Hill N A and Whaley K B 1995 *Phys. Rev. Lett.* **75** 1130
[8] Rama Krishna M V and Friesner R A 1991 *Phys. Rev. Lett.* **67** 629
[9] Wang L W and Zunger A 1994 *J. Phys. Chem.* **98** 2158
[10] Franceschetti A and Zunger A 1997 *Phys. Rev. Lett.* **78** 915
[11] Ogut S, Chelikowsky J R and Louie S G 1997 *Phys. Rev. Lett.* **79** 1770
[12] Kayanuma Y and Momiji H 1990 *Phys. Rev.* B **41** 10261
[13] J. Ferreyra M and Proetto C R 1999 *Phys. Rev.* B **60** 10672
[14] Tsu R, Ioriatti L, Harvey J F, Shen H and Lux R A 1993 *Mat. Res. Soc. Symp. Proc.* **283** 437
[15] Wang L W and Zunger A 1994 *Phys. Rev. Lett.* **73** 1039
[16] Jackson J D 1962 *Classical Electrodynamics* (New York: Wiley)
[17] Bolcatto P G and Proetto C R 1999 *Phys. Rev.* B **59** 12487
[18] Kumagai M and Takagahara T 1989 *Phys. Rev.* B **40** 12359
[19] Tran Thoai D B, Zimmermann R, Grudmann M and Bimberg D 1990 *Phys. Rev.* B **42** 5906
[20] Banyai L, Gilliot P, Hu Y Z and Koch S W 1992 *Phys. Rev.* B **45** 14136
[21] Stern F 1978 *Phys. Rev.* B **17** 5009
[22] Bastard G, Brum J A and Ferreira R 1991 *Solid State Phys.* **44** 229
[23] Bastard G 1988 *Wave Mechanics Applied to Semiconductor Heterostructures* (Les Ulis: Les Editions de Physique)
[24] Ferreyra J M and Proetto C R 1998 *Phys. Rev.* B **57** 9061
[25] Schiff L 1949 *Quantum Mechanics* (New York: McGraw-Hill)
[26] Yu P Y and Cardona M 1996 *Fundamentals of semiconductors: physics and material properties* (Berlin: Springer)
[27] Hermanson J 1966 *Phys. Rev.* B **150** 660
[28] Walter J P and Cohen M L1970 *Phys. Rev.* B **2** 1821
[29] Oliveira L E and Falicov L M 1986 *Phys. Rev.* B **34** 8676